Proceedings of the Sixth International Conference on
Railway Technology: Research, Development and Maintenance
Edited by: J. Pombo
Civil-Comp Conferences, Volume 7, Paper 9.8
Civil-Comp Press, Edinburgh, United Kingdom, 2024
ISSN: 2753-3239, doi: 10.4203/ccc.7.9.8

An Innovative Wheel Wear Model to Study the Profiles Evolution in Presence of Conformal Contact Conditions

L. Nencioni, E. Meli, A. Rindi and Z. Shi

**Department of Industrial Engineering of Florence (DIEF),
University of Florence
Italy**

Abstract

One of the main problems in railway and tramway systems, both dynamically (safety, comfort) and economically (planning of maintenance interventions, reduction of wheel and rail lifetime etc.), is represented by the wear of wheel and rail profiles, due to the wheel-rail interaction. The profile's shape variation, caused by wear and material removing, influence the dynamic behaviour of the vehicle and, in particular, the wheel-rail contact conditions. Hence, nowadays, one of the most important topics in the railway field is the development of a reliable and efficient wear model to predict the wheel and rail profiles evolution. For this reason, the aim of this work is the development of a new efficient wear model for the evaluation of the wheel and rail profile evolution based on an innovative wheel-rail conformal contact model.
More in detail, conformal contact conditions are really frequent in railway applications, particularly in sharp curves and, generally, in presence of worn profiles. Because all this reason, if an accurate wear assessment is required, this aspect cannot be neglected. In the proposed wear model, two separate blocks mutually interact: a multibody vehicle model for the dynamical analysis and a MATLAB/Simulink model for the wear evaluation. In the first one a multibody model of the vehicle, development in Simpack Rail, and an innovative and efficient conformal contact model based on an improvement of the Piotrowski classic contact model interact online during the dynamic simulations. Starting from the outputs of the dynamic simulations (position and shape of the contact patches, contact pressures, etc.), the wear model calculates the specific volume of removed material by wear through suitable experimental laws that correlate this volume to the friction power produced by the tangential contact

pressures. Finally, the new updated profiles of wheel and rail are obtained by subtracting the material removed from the old ones.

Keywords: conformal contact model, wear, non-Hertzian contact, wheel profile, multibody simulation, wheel-rail contact, railway vehicle.

1 Introduction

One of the issues in the railway field is the damage caused by wear, which deeply affects wheel and rail. In railway applications the estimation of wear at the wheel–rail interface is an important field of study, mainly correlated to the planning of maintenance interventions, vehicle stability and the possibility of carrying out specific strategies for the wheel and rail profiles optimization. For this reason, the development of an efficient and accurate wear model capable of predicting the evolution of wheel and rail profiles is one of the most important fields of study in railway engineering. One of the most important problem during the development of a wear model specifically designed for the multibody applications, is the wheel – rail contact model. More in details, many of the models that are available in literature [1] [2] to study the wheel and rail profiles evolution due to wear are based on the FASTSIM algorithm [3], where the normal problem is solved using Hertz theory [4], and the tangential problem is solved by an iterative strip algorithm. With this kind of approach, it is possible to solve the contact problem very quickly and efficiently, but this solution is based on some fundamental hypothesis, as flat and elliptical contact patch. For this reason, FASTSIM algorithm is not recommended in presence of conformal contact conditions. Furthermore, the complex problems arising from conformal contact patches are usually faced and investigated through Finite Element (FE) approaches. The FE methods are quite critical in terms of computational load and are very difficult to be used within multibody software to perform dynamic real-time simulation on large and complex scenarios. To extend the study of the wheel – rail contact and so to extend the study of the wheel and rail profiles evolution, even in presence of conformal contact conditions, the authors propose an innovative wheel and rail wear model based on an innovative and efficient conformal contact model. In this way the proposed model is able to evaluate the wheel and rail profile evolution even in presence of not flat and not elliptical contact patch and so in presence of conformal contact conditions.

2 Methods

The general layout of the proposed wear model developed in this research work is made up of two main parts (see Figure 1):

- the *dynamic system*;
- the *wear model*.

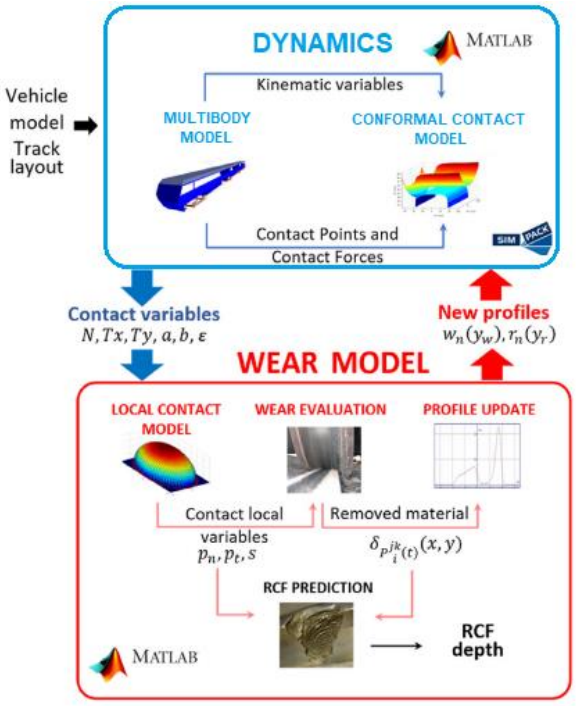

Figure 1: General architecture of the global model.

The dynamic block consists of a multibody model of the benchmark vehicle, built in Simpack Rail environment, and of a conformal contact model built in MATLAB/Simulink. During the dynamical simulation these models interact online creating a loop. Generally, the resolution of wheel-rail contact is divided into three phases:

- detection of contact points;
- calculation of normal pressure distribution;
- calculation of tangential pressure distribution.

Simpack Rail software already includes several wheel-rail contact models but, in this work, to extend the wear model even in presence of conformal contact conditions, an innovative conformal contact model has been used. Then, for each contact point, the model calculates contact forces (normal and tangential) and the global creepages of the contact patches. The global contact variables are then passed to the multibody model to carry on the simulation of the vehicle dynamics.

The wear model consists instead of three distinct phases:

- the *local contact model*;
- the *wear evaluation model*;
- the *profile update strategy*.

More in detail, the local contact model, based on the proposed and innovative conformal contact model, starting from the global contact variables (outputs of multibody simulation), evaluates the local contact variables (contact pressures and local creepages inside the curved contact patch) and divides the contact patch into adhesion area and slip area. Then, the distribution of removed material is calculated on the wheel and rail surface only within the slip area using an experimental law connecting the removal material to the energy dissipated by friction at the contact interface [5]. Finally, the wheel and rail worn profiles are obtained from the original ones through an innovative update strategy. The new updated wheel and rail profiles are then fed back as inputs to the vehicle model and the whole model architecture can proceed towards the next discrete step.

2.1 Multibody model of the vehicle

The benchmark vehicle chosen for this research is a generic italian driverless subway vehicle. It is a fixed-length trains and it consist of four carbodies and five bogies (four motorized and one trailer).

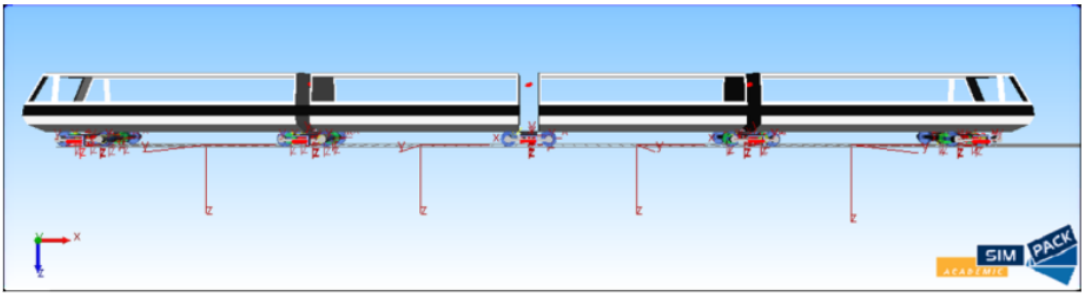

Figure 2: Multibody model of the chosen vehicle.

The bogie frames are made up of two articulated semi-frame connected each other by a particular spherical joint to ease the vehicle entry in sharp curves (see Figure 3). The multibody model (Figure 2) consists of several rigid bodies connected each other by means of appropriate elastic and damping elements. Particularly the vehicle is equipped with two suspension stages. Both the stages of suspensions have been modelled by means of viscoelastic force elements taking into account all the mechanical non linearities of the system (bumpstop clearance, dampers and rod behaviour).

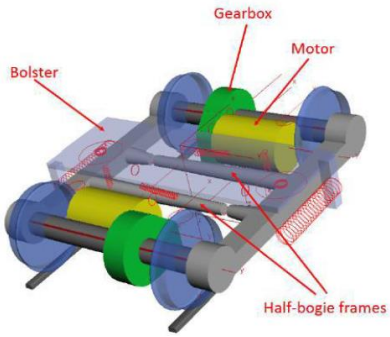

Figure 3: Architecture of the vehicle motor bogie.

2.2 The innovative conformal contact model

Different types of wheel-rail contact models can be found in literature. Excluding the finite element strategy, too slow to be implanted in multibody software, most of the approaches proposed are based on Hertz, Carter, Mindlin and Cattaneo theory and then are based on the half-space approach: they assume a concentrated contact and characteristic sizes of the bodies in contact large if compared to the size of the contact patch. In presence of conformal contact, really frequent in railway applications, this assumption is often violated, particularly in the cases of contact between flange root and rail gauge corner where none of standard contact models work satisfactorily and, more generally, in presence of worn profiles. The proposed contact model is specially developed for conformal contact: it is capable of computing large contact area comparable with wheel-rail typical bodies dimensions without assuming Hertzian hypothesis such elliptical shape, planar or symmetric contact patches.

The resolution of wheel-rail contact problem is divided in three phases:

- the *contact area detection*, based on an efficient algorithm;
- the *normal problem* resolution, based on an extension of the classic Piotrowski contact model;
- the *tangential problem* resolution, based on an extension of the classic FASTSTIM algorithm.

2.2.1 Normal contact model

More in detail, as said previously, the normal part of the contact problem is based on an extension of Piotrowski contact model [6], which is a good compromise between accuracy and numerical efficiency for the simulate of non elliptical, but planar contact. This model is based on the fundamental hypothesis that the real shape of the contact bodies in the contact patch are neglected and approximated through two elastic half-spaces; in this way the normal contact pressure $p_n(x,y)$ are correlated to the displacements along the vertical axis $w\,(x,y)$ by means the Cerruti-Bussinesq's influence function [6], as shown in Equation 1.

$$w(x,y) = \frac{1-\nu^2}{\pi E}\int_{A_c} \frac{p_n(x',y')}{\sqrt{(x-x')^2+(y-y')^2}}\, dA_c \tag{1}$$

where E is the Young's modulus and ν is the Poisson's modulus of the contact bodies material. At this point, following the Hertz solution [8], Piotrowski et al. [12] assume a semi – elliptical pressure distribution along the rolling direction, as follow:

$$p(x,y) = \frac{p_0}{x_l(0)}\int_{y_r}^{y_l}\int_{-x_l}^{x_l}\sqrt{{x_l}^2(y)-x^2}\; dx\, dy \tag{2}$$

where $x_l(y)$ is the distance along the rolling direction between the boundary of the

real contact area and a generical point (x, y) of the contact area, consequently $x_l(0)$ is the longitudinal semi – axis of the elliptical contact patch centred in the geometrical contact point (0,0) and p_0 is the maximum normal pressure value. By substituting Eq. (2) in Eq. (1) and assuming, as shown by the classic Piotrowski contact model that the rigid penetration $\delta = 2w(0,0) = 2w_0$, where w_0 is the bodies displacement in the geometrical contact point, it is possible to obtain the following expression of the maximum normal pressure p_0:

$$p_0 = \frac{x_l(0)\,\delta\,\pi\,E}{2(1-\nu^2)}\left(\int_{y_r}^{y_l}\int_{-x_l}^{x_l}\frac{\sqrt{{x_l}^2(y)-x^2}}{\sqrt{x^2+y^2}}\right)^{-1} \tag{3}$$

The extension of the Piotrowski normal contact model, to introduce the conformity effect is based on Blanco-Lorenzo's coefficients which are used by their authors to extend CONTACT in [7]. These are an extension of influence coefficients that are defined into the Kalker theory [8] to correlate displacement and applied load between a couple of elastic half-spaces.

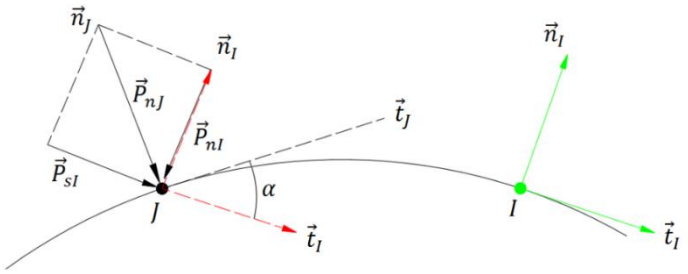

Figure 4: Influence function coefficientes correction.

As shown in the Figure 4, the load applied at a given point *J*, in A_c is decomposed in the $\vec{t}_I$ (tangential) and $\vec{n}_I$ (normal) directions associated to the point *I* where the displacements are observed, according to Equation (4):

$$\vec{P}_{nJ} = \vec{P}_{nI} + \vec{P}_{tI} = \left|\vec{P}_{nJ}\right| \cdot cos(\alpha) \cdot \vec{n}_I + \left|\vec{P}_{nJ}\right| \cdot sin(\alpha) \cdot \vec{t}_I \tag{4}$$

Following the reasonament in [19] the influence coefficients for conformal geometries are approximated through a combination of the influence coefficients of the half-space, according to Blanco – Lorenzo [7]. More in detail, the Piotrowski's model extension needs using only one corrected influence coefficient, that is $B_{nn_{conf}}$, as reported in Equation 5.

$$B_{nn_{conf}} \approx B_{nn} \cdot cos\,\alpha - B_{nt} \cdot sin\,\alpha \tag{5}$$

Introducing the $B_{nn_{conf}}$ influence coefficient (Equation 5) into the Piotrowski based classic Cerruti-Bussinesq's influence function it is possible to obtain a new influence function that is now also valid for conformal contact conditions:

$$w(x,y) = \frac{\nu+1}{\pi E}\int_{A_c}\left(\frac{p_n(x',y')\,cos(\alpha)\,(1-\nu)}{\sqrt{(x-x')^2+(y-y')^2}} + \frac{p_n(x',y')\,sin(\alpha)\,Ky}{(x-x')^2+(y-y')^2}\right)dx'dy' \tag{6}$$

Where $cos(\alpha)$ and $sin(\alpha)$ are functions of the curvature of the contact patch, and K is a function of the wheel and rail material characteristics. At this point, it is important to observe that, when the contact patch is conformal it is fundamental to change the coordinates where the problem is studied to take into account the conformity effect and the surface curvature. In order to develop an efficient and realistic model when the contact patch is non flat and it is non small with respect to the curvature radii of the contacting bodies it is useful to introduce the following variables:

$$\begin{cases} x \to x^r \\ y \to s^r \end{cases} \tag{7}$$

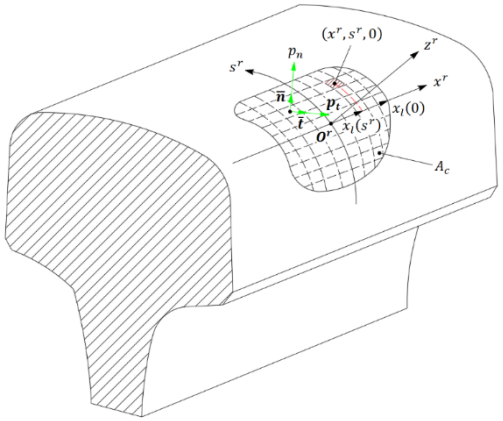

Figure 5: Rail contact patch reference system with curvilinear abscissa.

where s^r, as shown in Figure 5, is the curvilinear abscissa of the rail profile. For this reason, the Equation (6) can be rewritten as follows:

$$w(x^r,s^r) = \frac{\nu+1}{\pi E}\int_{A_c}\left(\frac{p_n(x^{r\prime},s^{r\prime})\,cos(\alpha)\,(1-\nu)}{\sqrt{(s^r-s^{r\prime})^2+(x^r-x^{r\prime})^2}} + \frac{p_n(x^{r\prime},s^{r\prime})\,sin(\alpha)\,Ks^r}{(s^r-s^{r\prime})^2+(x^r-x^{r\prime})^2}\right)dA_c \tag{8}$$

At this point, according to Piotrowski's procedure [6], the new influence function has been used to evaluate the maximum normal pressure p_0 in presence of conformity conditions, al follow:

$$p_0 = \frac{\pi E\delta {x^r}_l(0)}{2(1+\nu)}\left\{\int_{A_c}\left(\frac{\sqrt{x^r(s^r)^2 - x^{r2}}\cos(\alpha)\,(1-\nu)}{\sqrt{x^{r2}+s^{r2}}} + \frac{\sqrt{x^{r2}(s^r)-x^{r2}}\sin(\alpha)\,Ks^r}{x^{r2}+s^{r2}}\right)dx'dy'\right\}^{-1} \tag{9}$$

2.2.1 Tangential contact model

Regarding the tangential problem, in this work an extension of FASTSIM algorithm [3] has been proposed (basing on the Kalker Book of Tables for non-Hertzian model [9], to extend the algorithm even to non elliptical and problems. The KBTNH model approximates the non elliptical and non symmetrical planar contact patch by a single double-elliptical contact area, as it is possible to see in Figure 6.

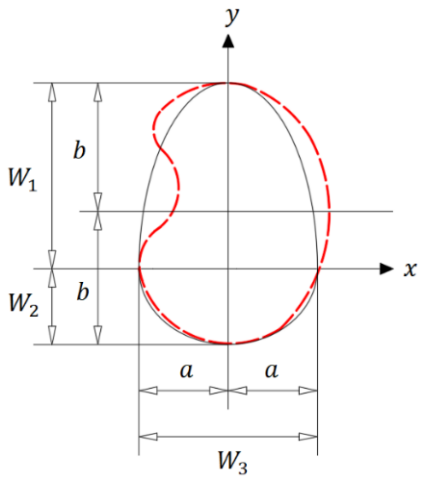

Figure 6: Double elliptical contact (SDEC) patch of the KBTNH algorithm.

More in details the idea of the KBTNH algorithm is to bring back the non elliptical, non symmetrical and non planar contact patch to a single double elliptical contact (SDEC) patch that, as shown in Figure 6, is characterized by two fundamental dimensions:

$$a = \sqrt{\frac{A_c}{\pi}\frac{W_3}{(W_1 + W_2)}} \tag{10}$$

$$b = \sqrt{\frac{A_c}{\pi}\frac{(W_1 + W_2)}{W_3}} \tag{11}$$

where A_c is the area of the contact patch, and W_1, W_2, W_3 are the dimensions depicted in Figure 10. In this way the conformal contact patch is bring back to a SDEC region where it is possible to evaluate the output of the tangential problem using an extension of the FASTSIM algorithm based on the KBTNH model [9]. As a result of the change of coordinates, described in the previous section, one necessary to study the tangential contact problem in presence of a conformal contact patch, the FASTSIM algorithm has been updated as described below. One of the most important step during the application of the FASTSIM algorithm is the discretization of the contact patches

using a grid (cell size in the longitudinal direction $\Delta x \rightarrow \Delta x^r$ and $\Delta y \rightarrow \Delta s^r$ in lateral direction), as shown in Figure 7.

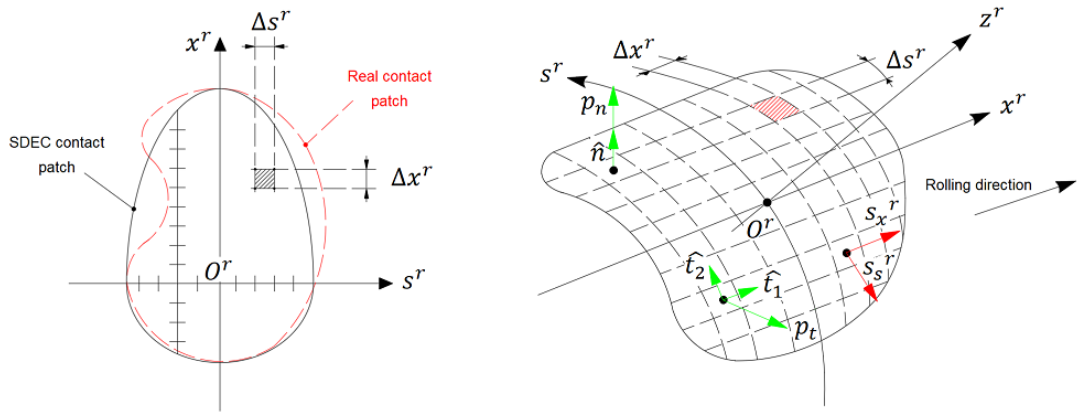

Figure 7: FASTSIM (KBTNH) algorithm conformal contact patch discretization.

At this point the standard FASTIM algorithm [3] is used for each of the *j-th* stripes of the no-planar contact patch of width Δs^r to calculate the tangential stresses $\boldsymbol{p_t}(x^r, s^r)$.

2.3 The wear model

The wear model consists of three distinct phases:

- the *local contact model*;
- the *wear evaluation model*;
- the *profile update strategy*.

More in detail, the local contact model, based on the proposed and innovative conformal contact model, starting from the global contact variables (outputs of multibody simulation), evaluates the local contact variables (contact pressures and local creepages inside the curved contact patch) and divides the contact patch into adhesion area and slip area. Then, the distribution of removed material is calculated on the wheel and rail surface only within the slip area using an experimental law connecting the removal material to the energy dissipated by friction at the contact interface [5]. Finally, the wheel and rail worn profiles are obtained from the original ones through an innovative update strategy. The new updated wheel and rail profiles are then fed back as inputs to the vehicle model and the whole model architecture can proceed towards the next discrete step.

2.3.1 The wear evaluation

Starting from the local contact variables estimated in every point of the contact patch grid, it is possible to evaluate the specific volume of removed material on the wheel (in $[mm^3/(m \cdot mm^2)]$) $\delta_{P_{wi}^j(t)}(x^r, s^r)$ for unit of distance travelled by the vehicle (in m)and for unit of contact surface (in mm^2). For this reason, an experimental

relationship between the volume of removed material and the dissipated energy at the contact interface has been used. More in detail, knowing the tangential pressure distribution $\boldsymbol{p_t}(x^r, y^r)$ and local rigid sliding $\boldsymbol{s}(x^r, y^r)$, the Wear Index $I_w(x^r, s^r)$ (expressed in $[N/mm^2]$) which represents the frictional power generated by the tangential contact pressure distribution, can be evaluated as follow:

$$I_w = \frac{\boldsymbol{p_t}(x^r, s^r) \cdot \boldsymbol{s}(x^r, s^r)}{\mathrm{V}} = \boldsymbol{p_t}(x^r, s^r) \cdot \boldsymbol{\gamma}(x^r, s^r) \tag{12}$$

where V is the longitudinal velocity of the vehicle and $\boldsymbol{\gamma}(x^r, s^r)$ the local creepages. This parameter is then connected to another fundamental parameter, the wear rate $K_w(x^r, s^r)$ (expressed in $[\mu g/(m \cdot mm^2)]$), that represents the removed volume of material, from the wheel surface, for unit of distance travelled by the vehicle and for unit of contact patch surface. The two indexes are correlated by means of a heuristic law based on dedicated experimental wear tests [10], as reported below:

$$K_w(x^r, s^r) = \begin{cases} 5.3 \cdot I_w(x^r, s^r) \quad if \quad I_w(x^r, s^r) < 10.4 \\ 55.1 \quad if \quad 10.4 \leq I_w(x^r, s^r) < 77.2 \\ 61.9 \cdot I_w(x^r, s^r) - 4778.7 \quad if \quad I_w(x^r, s^r) \geq 77.2 \end{cases} \tag{13}$$

After obtaining the wear rate $K_w(x^r, s^r)$ the specific volume of removed material on wheel can be calculated as:

$$\delta_{P^j_{wi}(t)}(x^r, s^r) = K_w\big(I_w(x^r, s^r)\big) \cdot \frac{1}{\rho} \tag{14}$$

where ρ is the material density.

2.3.2 The profile update strategy

In this subsection a summary of the profile update strategy will be provided. For a full description of the approach the reader can refer to the works available in literature [1,2]. After obtaining the amount of worn material, the wheel profile has to be updated to be used as inputs for the next step of the iterative process. The update strategy requires some integration and average operations in order to remove the numerical noise affecting the distributions $\delta_{P^j_{wi}(t)}(x^r, s^r)$ and to calculate the total quantities of removed material due to wear $\Delta^w(s_w)$ (expressed in mm), where s_w is the natural abscissas of the wheel profile (see Figure 8).

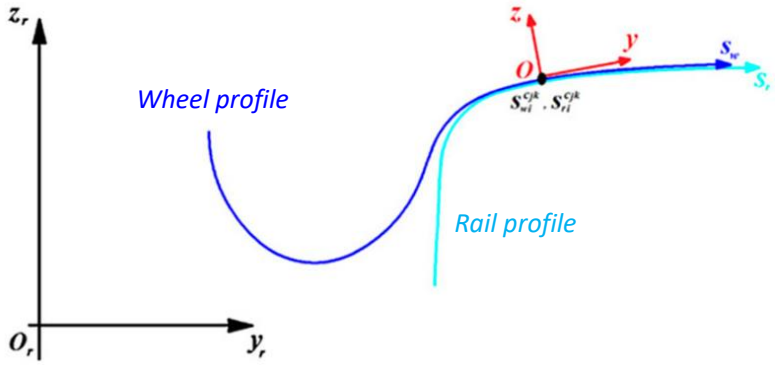

Figure 8: Wheel profile curvilinear abscissa.

More in detail, the update strategy can be summarized as follow:

- *longitudinal integration* – all the wear contributes inside the contact patch are summed along the longitudinal direction and this quantity is averaged over the whole longitudinal development of the wheel surface:

$$\delta_w^{tot}(s^r) = \frac{1}{2\pi \cdot w(z_w)} \int_{-b(s^r)}^{+b(s^r)} \delta_{P_{wi}^j(t)}(x^r, s^r)\, dx^r \tag{15}$$

where $w(z_w)$ is the wheel radius evaluated in the geometrical contact point;

- *track integration* – this integration over the track length adds all the wear contributions coming from the dynamic simulation to calculate the depth of removed material from the wheel surface:

$$\Delta^w(s_w) = \int_{x_{start}}^{x_{end}} \delta_w^{tot}(s^r) \cdot V(t)\, dt \tag{16}$$

- *sum of the contact points contributes* – all the wear contributes of each *i-th* contact point are summed as follow:

$$\Delta^w(s_w)^{tot} = \sum_{i=1}^{N} \Delta^w(s_w)^i \tag{17}$$

- scaling – since normally travelled distances of thousands of kilometres are needed to obtain measurable wear effects, an appropriate scaling procedure is required to reduce the simulated track length with a consequent lighter computational effort. More in detail, the total mileage km_{tot} travelled by the vehicle during the wheel profile life has been subdivided into constat steps of length km_{step} (see Figure 9).

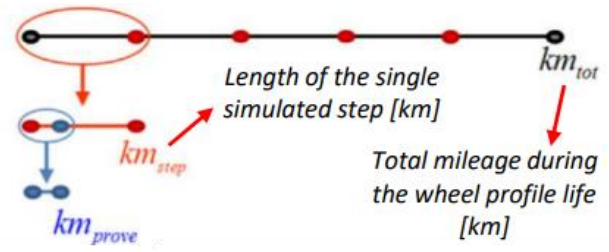

Figure 9: Scaling procedure architecture.

In this research, an adaptive strategy has been chosen to update the wheel and rail profiles: the approach imposes a threshold value on the maximum of the removed material at each discrete step. The removed material on the wheel is proportional to the distance travelled by the vehicle on each step. Thus, the material removed on the wheel has to be scaled according to the following law:

$$\Delta^w(s_w)^{tot}\frac{km_{step}}{l_{track}} = \Delta^w(s_w)^{scal} \tag{18}$$

Where km_{step} is calculated in an adaptive way setting a threshold value D^w_{step} on the maximum of the removed material quantity on the wheel at each discrete step, as follow:

$$km_{step} = km_{prove}\frac{D^w_{step}}{max(\Delta^w(s_w)^{tot})} \tag{19}$$

With $max(\Delta^w(s_w)^{tot})$ that corresponds to the maximum value of wear depth obtained from the simulation before the scaling operation, and km_{prove} is the mileage travelled by the vehicle during the dynamic simulations.

3 Results

According to the update strategy described previously, the threshold value on the maximum thickness of material removed by wear on the wheels at each wheel discrete step has been chosen equal to 0.4 mm. Therefore, when the removed material reaches this quantity, a discrete step finishes and the whole procedure passes to the following discrete step.

3.1 Simulated test case

In order to evaluate the output of the whole model a generic Italian subway line has been considered. More in detail, starting from a classic complete subway line a specific statistical approach has been chosen, in order to reduce the simulation time. The complete chosen track has been divided in five different classes, in function of the curved radii, and for each class a specific statistical weight has been introduced.

In conclusion, only five curved track section have been simulated, as it is possible to see in Table 1.

Track class	***Total length*** [m]	***Statistical weight*** [m]
Straight Track class 1 ($R = \infty$)	8870	0.72
Curved Track class 2 ($100\ m \leq R < 200\ m$)	1293	0.1
Curved Track class 3 ($200\ m \leq R < 300\ m$)	1744	0.14
Curved Track class 4 ($300\ m \leq R < 500\ m$)	331	0.03
Curved Track class 5 ($500\ m \leq R < 1000\ m$)	141	0.01

Table 1: Track sections statistical weights.

3.2 Model preliminary results

The reference parameters FH (flange height), FT (flange thickness) and QR quota are capable of estimating the wheel profile evolution due to wear without necessarily knowing the whole profile shape (see Figure 10).

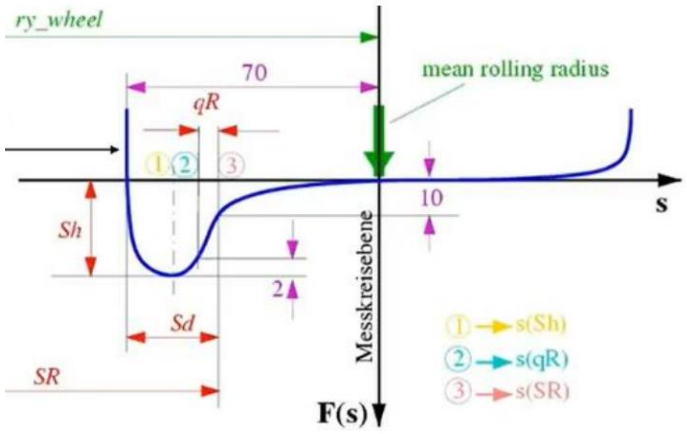

Figure 10: Wheel wear reference parameters.

For this reason, the evolution of wear control parameters, obtained from the dynamic simulations have been compared with the output of a classic non conformal contact model, in order to evaluate the conformity effect on the wheel profile evolution.

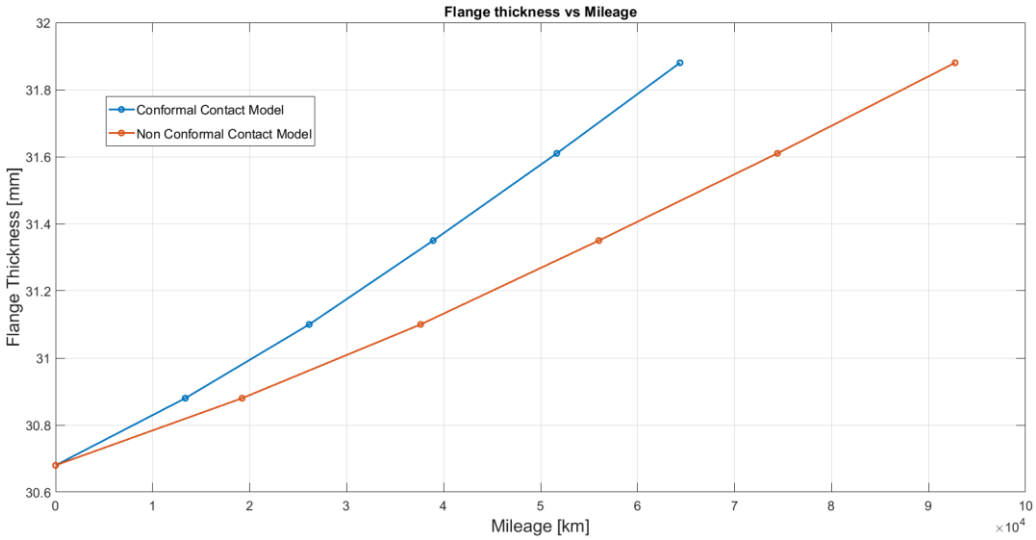

Figure 11: Flange thickness vs mileage.

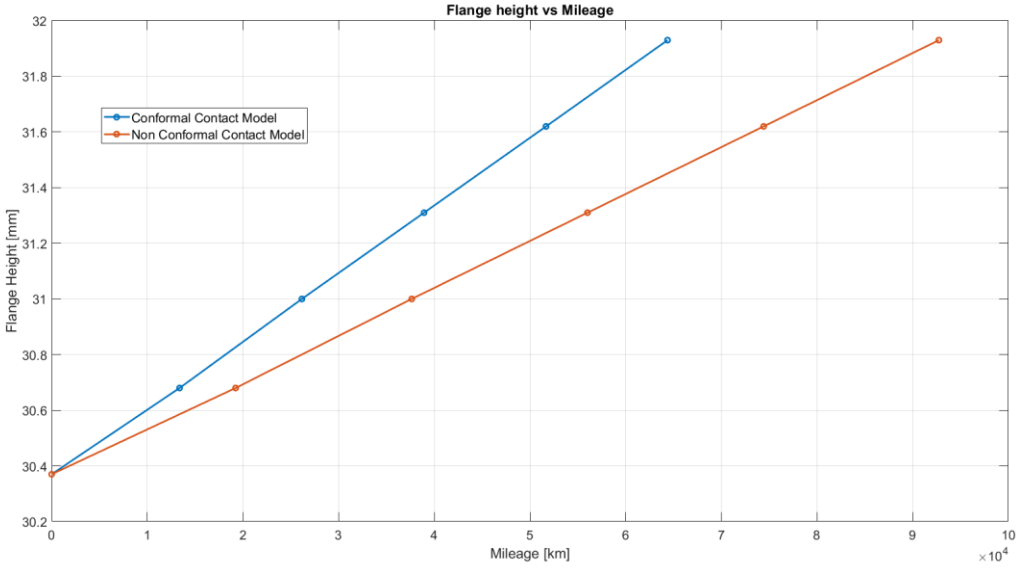

Figure 12: Flange height vs mileage.

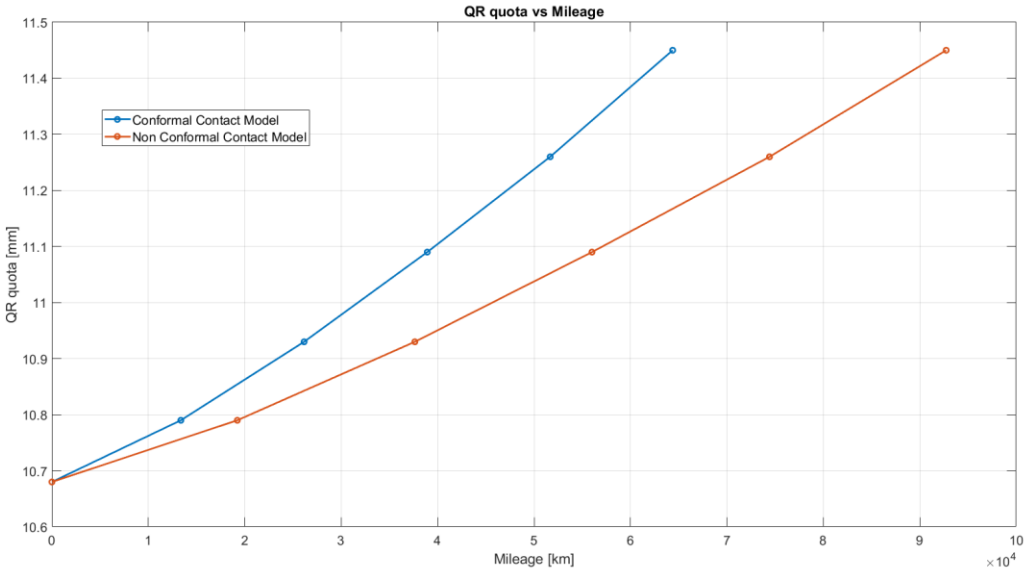

Figure 13: QR quota vs mileage.

The FT quota progress is represented in Figure 11 as a function of the mileage and shows how the flange height increases and the wear is mainly localized on the wheel tread. The progress of FH dimension is shown in Figure 12, and furthermore, in Figure 13 is shown the QR trend. More in detail, from the results, it is possible to evidence that the conformal contact model tends to overestimate the wheel wear evolution respect to the non-conformal contact model, as it is also possible to see in Figure 14, where the wheel profile evolution, has been plotted to the same mileage (about 38'000 km), respectively with a conformal and non-conformal contact model.

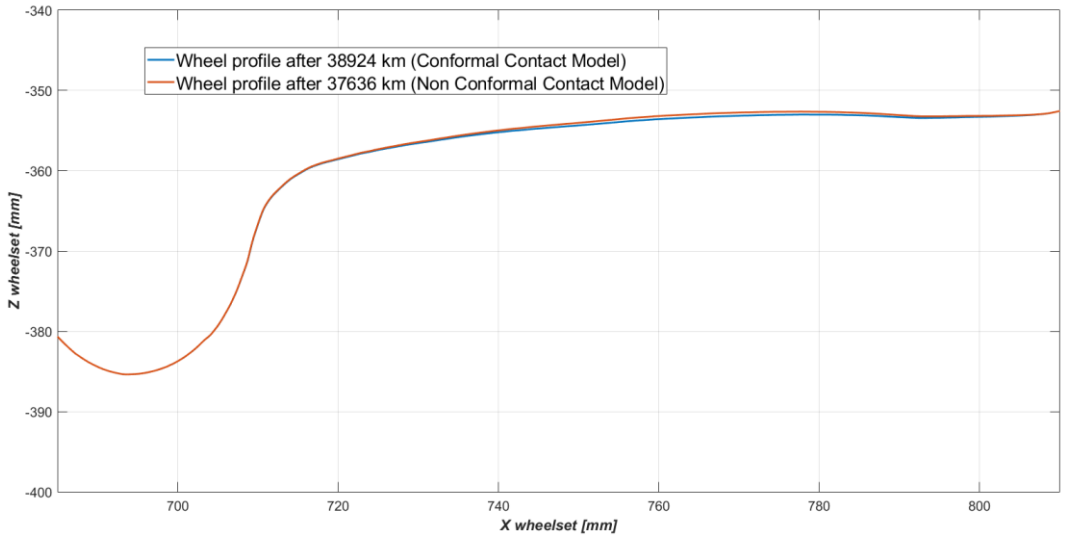

Figure 14: Wheel profile evolution with a CCM ad with a NCCM.

4 Conclusions and Contributions

In this work the Authors have presented a complete model for the wheel wear prediction in railway application, specially developed for conformal contact case really frequent in railway applications and whose cannot be neglected in order to obtain an accurate wear prediction. The whole model is made up of two parts which mutually interact during the simulation running. The first one evaluates the vehicle dynamics and comprises both the multibody model of the vehicle implemented in Simpack and the innovative wheel–rail conformal contact model. The contact model is composed by the contact area detection phase and the force calculation phase that represent the core of the proposed approach; it is capable of evaluating the contact pressures and the tangential stresses overcoming the standard Hertzian hypothesis for the calculation of the contact points and of the contact forces. The normal problem has been treated by means of an extension of the Piotrowski approach to consider the not planar contact patch, typical situation occurring in wheel flange-rail corner conformal contact and in the presence of wheel and rail worn profiles. The tangential problem has been treated as an extension of the classic FASTSIM algorithm based on the KBTNH algorithm. The second part of the whole model is the wear model which, starting from the outputs of the multibody simulations, evaluates the amount of material to be removed due to wear and updates the wheel and rail profiles. The interaction between the two parts is not a continuous time process but occurs at discrete steps; consequently the evolution of the wheel and rail geometry is described through several intermediate profiles. The results obtained by the comparison between the proposed conformal contact wear model and a classic wear model based on a non-conformal contact model showed that the conformity effect is able to speeding up the wheel profile evolution due to higher creep and tangential pressure peaks. In terms of future development, the obtained results will be compared with experimental data in order to validate the proposed and innovative wheel wear model.

References

[1] M. Ignesti, M. Malvezzi, L. Marini, E. Meli, A. Rindi. “Development of a wear model for the prediction of wheel and rail profile evolution in a railway system.” Wear 284-285 (2012) 1–17.

[2] F. Braghin, R. Lewis, R.S. Dwyer-Joyce, S. Bruni. “A mathematical model to predict railway wheel profile evolution due to wear.” Wear 261, pp. 1253–1264, 2006.

[3] J.J. Kalker. “A fast algorithm for the simplified theory of rolling contact.” Vehicle System Dynamics, Vol. 11, pp. 1–13, 1982.

[4] Hertz. H.: The contact of elastic solids, Journal fur Die Reine und Angewandte Mathematik 92 (1881) 156-171.

[5] E. Butini, L. Marini, E. Meli, S. Panconi, A Rindi, B. Romani. “A New Wear Model Considering Wheel-Rail Conformal Contact.” ICRT 2017.

[6] J.Piotrowski, W.Kik. “A simplified model of wheel/rail contact mechanics for non-Hertzian problems and its application in rail vehicle dynamic simulation.” Vehicle System Dynamics, Vol.46, Nos. 1-2, January –February 2008, 27 –48.
[7] J. Blanco Lorenzo, J. Santamaria, E. Vadillo, N. Correa. “On the influence of conformity on wheel-rail rolling contact mechanics.” Tribology International 103 (2016), 647-667.
[8] J.J. Kalker. “Three dimensional Elastic Bodies in Rolling Contact Solid Mechanics and its Applications.” 1990.
[9] J. Piotrowski, B. Liu, S. Bruni. “The Kalker Book of tables for non-Hertzian contact of wheel and rail.” Vehicle System Dynamics 55-6, 875-90.
[10] Z. Shi, L. Nencioni, E. Meli, H. Ding, W. Wang, A. Rindi. “Effect of material hardness ratio on wear and rolling contact fatigue: Development and validation of new laws.” Wear 514-515 (2023).